Detection of Lesions in Mesial Temporal Lobe Epilepsy by Using MR Fingerprinting

*Congyu Liao, BS** • *Kang Wang, MD** • *Xiaozhi Cao, BS* • *Yueping Li, MS* • *Dengchang Wu, MD, PhD* • *Huihui Ye, PhD* • *Qiuping Ding, MS* • *Hongjian He, PhD* • *Jianhui Zhong, PhD*

From the Center for Brain Imaging Science and Technology, Key Laboratory for Biomedical Engineering of Ministry of Education, College of Biomedical Engineering and Instrumental Science (C.L., X.C., Y.L., H.Y., Q.D., H.H., J.Z.), Department of Neurology, The First Affiliated Hospital (K.W., D.W.), State Key Laboratory of Modern Optical Instrumentation, College of Optical Science and Engineering (H.Y.), and Center for Innovative and Collaborative Detection and Treatment of Infectious Diseases (J.Z.), Zhejiang University, 38 Zheda Rd, Hangzhou, Zhejiang 310027, China; and the Department of Imaging Sciences, University of Rochester, Rochester, NY (J.Z.).
Received September 8, 2017; revision requested November 10; revision received March 12, 2018; accepted March 28. **Address correspondence to** J.Z. (e-mail: *jzhong3@gmail.com*).

Study supported by National Natural Science Foundation of China (61701436, 81201007, 81401473, 91632109), the Doctoral Fund of Ministry of Education of China (20120101120070), and the Fundamental Research Funds for the Central Universities of China (2017QNA5016).

*C.L. and K.W. contributed equally to this work.

Conflicts of interest are listed at the end of this article.
See also the editorial by Prayer in this issue.

Radiology 2018; 288:804–812 • https://doi.org/10.1148/radiol.2018172131 • Content code: NR

Purpose: To improve diagnosis of hippocampal sclerosis (HS) in patients with mesial temporal lobe epilepsy (MTLE) by using MR fingerprinting and compare with visual assessment of T1- and T2-weighted MR images.

Materials and Methods: For this prospective study performed between April and November 2016, T1 and T2 maps were obtained and tissue segmentation performed in consecutive patients with drug-resistant MTLE with unilateral or bilateral HS. T1 and T2 maps were compared between 33 patients with MTLE (23 women and 10 men; mean age, 32.6 years; age range, 16–60 years) and 30 healthy participants (20 women and 10 men; mean age, 28.8 years; age range, 18–40 years). Differences in individual bilateral hippocampi were compared by using a Wilcoxon signed rank test, whereas the Wilcoxon rank-sum test was used for difference analysis between healthy control participants and patients with MTLE.

Results: The diagnosis rate (ie, ratio of HS diagnosed on the basis of a 2.5-minute MR fingerprinting examination compared with standard methods: MRI, electroencephalography, and PET) was 32 of 33 (96.9%; 95% confidence interval: 84.9%, 100%), reflecting improved accuracy of diagnosis ($P = 1.92 \times 10^{-12}$) over routine MR examinations that had a diagnostic rate of 23 of 33 (69.7%; 95% confidence interval: 51.5%, 81.6%). The comparison between atrophic and normal-appearing hippocampus in 33 patients with MTLE and healthy control participants demonstrated that both T1 and T2 values in HS lesions were higher than those of normal hippocampal tissue of healthy participants (T1: 1361 msec ± 85 vs 1249 msec ± 59, respectively; T2: 135 msec ± 15 vs 104 msec ± 9, respectively; $P < .0001$).

Conclusion: MR fingerprinting allowed for multiparametric mapping of temporal lobe within 2.5 minutes and helped to identify lesions suspicious for HS in patients with MTLE with improved accuracy.

Online supplemental material is available for this article.

Mesial temporal lobe epilepsy (MTLE) is the most common form of focal epilepsy in adolescents and young adults, characterized by recurrent spontaneous seizures that originate from the medial portion of the temporal lobe (1). Hippocampal sclerosis (HS) is the leading cause of MTLE and it accounts for about 40% of adult patients with epilepsy (2).

HS commonly demonstrates high signal intensity on T2-weighted images (3) and unilateral MTLE can often be detected by comparing two sides of hippocampi. Fluid-attenuated inversion recovery (FLAIR) sequences have been shown to be helpful in diagnosing mesial temporal sclerosis (4). Another tool for MRI analysis of HS is hippocampal volumetric measurements (5). Atrophy of the hippocampus can be detected by measuring hippocampal volume. In addition, other postprocessing methods such as voxel-based morphometry (6) of T1-, T2-, and diffusion-weighted imaging have been applied to improve the sensitivity of visual MRI analysis (7–10). However, routine MRI evaluation of patients with MTLE is generally on the basis of the assumption that the contralateral hippocampus is healthy. This implies that a visual comparative hippocampal assessment is likely to miss patients with bilateral MTLE with little or no volume loss or patients with unilateral MTLE and subtle T2 signal hyperintensity.

Quantitative T1- and T2-weighted imaging may help to recognize the subtle changes of tissue in patients with MTLE. Previous relaxometry studies of epilepsy patients demonstrated that both T1 and T2 values of epileptic focus are longer in patients with epilepsy compared with healthy control participants, which may be correlated with hippocampal gliosis and neuronal cell loss (11–13). However, quantitative imaging methods with high accuracy (3) such as inversion-recovery sequences (for T1 mapping) and spin-echo sequences (for T2 mapping) are rarely used in clinical applications because of their long acquisition time.

A recently proposed MR framework (14), referred to hereafter as MR fingerprinting, enables rapid and

Abbreviations

HS = hippocampal sclerosis, MTLE = mesial temporal lobe epilepsy

Summary

Within 2.5 minutes, MR fingerprinting identifies suspicious hippocampal sclerosis in patients with mesial temporal lobe epilepsy with improved accuracy over visual assessment of T1- and T2-weighted MR images.

Implications for Patient Care

- Within a short acquisition time of 2.5 minutes, MR fingerprinting identifies suspicious hippocampal sclerosis lesions in patients with mesial temporal lobe epilepsy.
- MR fingerprinting shows improved accuracy and sensitivity compared with visual assessment of T1-and T2-weighted MR images in patients with epilepsy.
- MR fingerprinting could potentially aid multimodal quantitative mapping and aid clinicians in diagnostic decision making for patients with epilepsy.

simultaneous multiple parametric mapping of T1, T2, and proton density. Some related work has shown the potential to extract useful clinical information in cardiac (15), abdominal (16), and quantitative tumor imaging (17,18). Furthermore, the relaxometry information obtained at MR fingerprinting can be used for tissue-fractional segmentation (14,19,20), which can aid in improving the accuracy and sensitivity of lesion detection.

In our study, MR fingerprinting was used to quantitatively investigate the subtle changes in HS lesions of patients with MTLE, and to compare the sensitivity and specificity of the MR fingerprinting method to the visual inspection with T1- and T2-weighted images.

Materials and Methods

Participants

On the basis of clinical history, manifestation, and interictal scalp electroencephalography, 45 patients with probable drug-resistant MTLE were imaged by using a clinical MRI protocol. All patients were consecutively recruited from the epilepsy clinic of Zhejiang University (Hangzhou, Zhejiang Province, China) between April 1 and November 30, 2016. Our prospective study was approved by the medical research ethics committee and the institutional review board, and all personnel involved had training and certification for conducting human studies. Written informed consent was obtained from each participant or from a legal representative.

The patient selection flowchart is shown in Figure 1. We excluded 12 patients. The inclusion criteria, exclusion criteria, and details of patient clinical information are provided in Appendix E1 (online).

As a control group, 30 age- and sex-matched healthy volunteers (20 women and 10 men; age range, 18–40 years; mean age, 28.8 years) were recruited from the local community from December 2015 to November 2016. All participants were older than 18 years and in good health, without a history of neurologic or psychiatric illness or history of intake of neuropsychiatric drugs. The MRI data of healthy

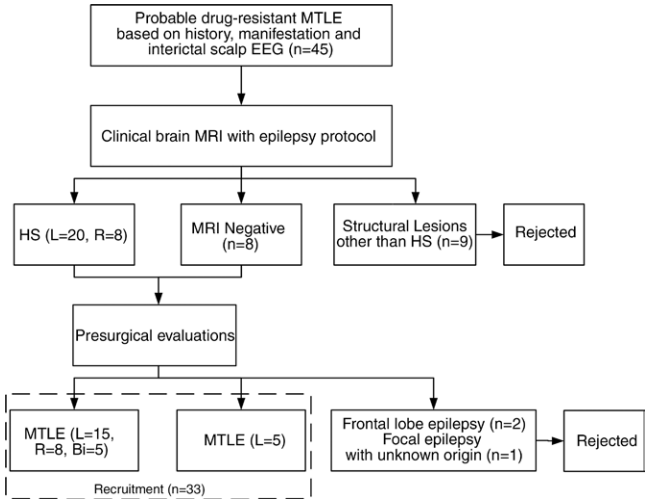

Figure 1: Patient selection flowchart. Bi = bilateral, EEG = electroencephalography, HS = hippocampal sclerosis, L = left, MTLE = mesial temporal lobe epilepsy, R = right.

volunteers were acquired by the same imaging protocol used in the patient examinations.

Data Acquisition and Image Reconstruction

MR measurements were performed on a 3.0-T imager (Magnetom Prisma; Siemens Healthineers, Erlangen, Germany) with a 20-channel head coil, and the total image acquisition time for each participant was about 18 minutes. The imaging protocol is in Table 1. Details of the imaging protocol are also provided in Appendix E1 (online). Briefly, after conventional fluid-attenuated inversion recovery, T1- and T2-weighted imaging, and two-dimensional MR fingerprinting (21) with sliding-window reconstructions (22) were performed in all participants, T1 and T2 maps were generated. Figure 2a shows the procedure of MR fingerprinting acquisition for each participant.

Identification of Components Suspicious for HS Lesions

MR fingerprinting can help to estimate the intravoxel tissue component fractions (19,20). In our study, MR fingerprinting data from the same patients were used for tissue-fraction segmentation and were regarded as a marker suspicious for HS lesions by using regularized tissue-fraction MR fingerprinting (23). The signal equation of regularized tissue-fraction MR fingerprinting is as follows:

$$\hat{\mathbf{w}} = \underset{\mathbf{w}}{\operatorname{argmin}} \left\| \mathbf{S}_{voxel} - \mathbf{D}\mathbf{w} \right\|^2 \; s.t. \{ \sum_{n=1}^{N} \mathbf{w}(n) = 1, \mathbf{w}(n) \in [0,1] \} ,$$

where the S_{voxel} represents the acquired signal curve of each voxel, D is the signal evolution of tissue components that were precalculated by using the extended phase-graph algorithm, *s.t.* is subject to, Σ is summation operator, n is the index of components, ε is element of, *argmin* is argument of the minimum, and w is the potential fraction group with components N. The optimization problem of the equation can be solved by using least-squares analysis with an additional con-

Table 1: MRI Protocol

Sequence	TR/TE (msec)	Field of View (mm)	Spatial Resolution (mm)	Section Thickness (mm)	No. of Sections	Imaging Time (min)
Localizer	3.1/1.4	260 × 260	1.60 × 1.60	1.6	3	0:12
3D T1-weighted MPRAGE	2300/2.3	240 × 240	0.93 × 0.93	0.93	192	6:18
Coronal 2D T2-weighted fast spin echo	6000/100	220 × 220	0.43 × 0.43	4.0	25	2:06
Transverse 2D T2-weighted fast spin echo	6000/100	220 × 220	0.43 × 0.43	4.0	25	2:06
Coronal FLAIR	8800/130	230 × 230	0.90 × 0.90	4.0	24	2:56
Coronal 2D MR fingerprinting	12–15/2.5	240 × 240	1.20 × 1.20	3	20	2:30
Transverse 2D MR fingerprinting	12–15/2.5	240 × 240	1.20 × 1.20	3	20	2:30

Note.—The total acquisition time was 17:58 minutes. 2D = two-dimensional, 3D = three-dimensional, FLAIR = fluid-attenuated inversion recovery, MPRAGE = magnetization-prepared rapid gradient echo, TE = echo time, TR = repetition time.

straint that takes the values of fractions and then normalizes them to the summation of 1.

Figure 2b shows steps of regularized tissue-fractional mapping on the basis of MR fingerprinting data. Detailed steps for detection of HS lesions on the basis of MR fingerprinting–defined components suspicious for lesions are provided in Appendix E1 (online).

Diagnosis of HS Patients

HS was defined at radiologic imaging by hippocampal atrophy and higher signal intensity of hippocampi on T2-weighted images primarily by using side-by-side visual comparison. The neuroradiologists examined the images obtained from the epilepsy MRI protocol (T1-weighted magnetization-prepared rapid gradient echo, two-dimensional axial, and coronal T2-weighted fluid-attenuated inversion recovery images) and focused on the size, shape, volume norms, and fluid-attenuated inversion recovery signal in hippocampi. Other minor findings associated with HS including dilatation of the temporal horns, loss of hippocampal head interdigitations, blurry gray and white matter demarcation in the temporal pole, and atrophy of the fornix were also taken into consideration. Regarding patients who were negative for HS at MRI reported by the neuroradiologists, hippocampal volumetry was routinely performed compared with healthy subjects.

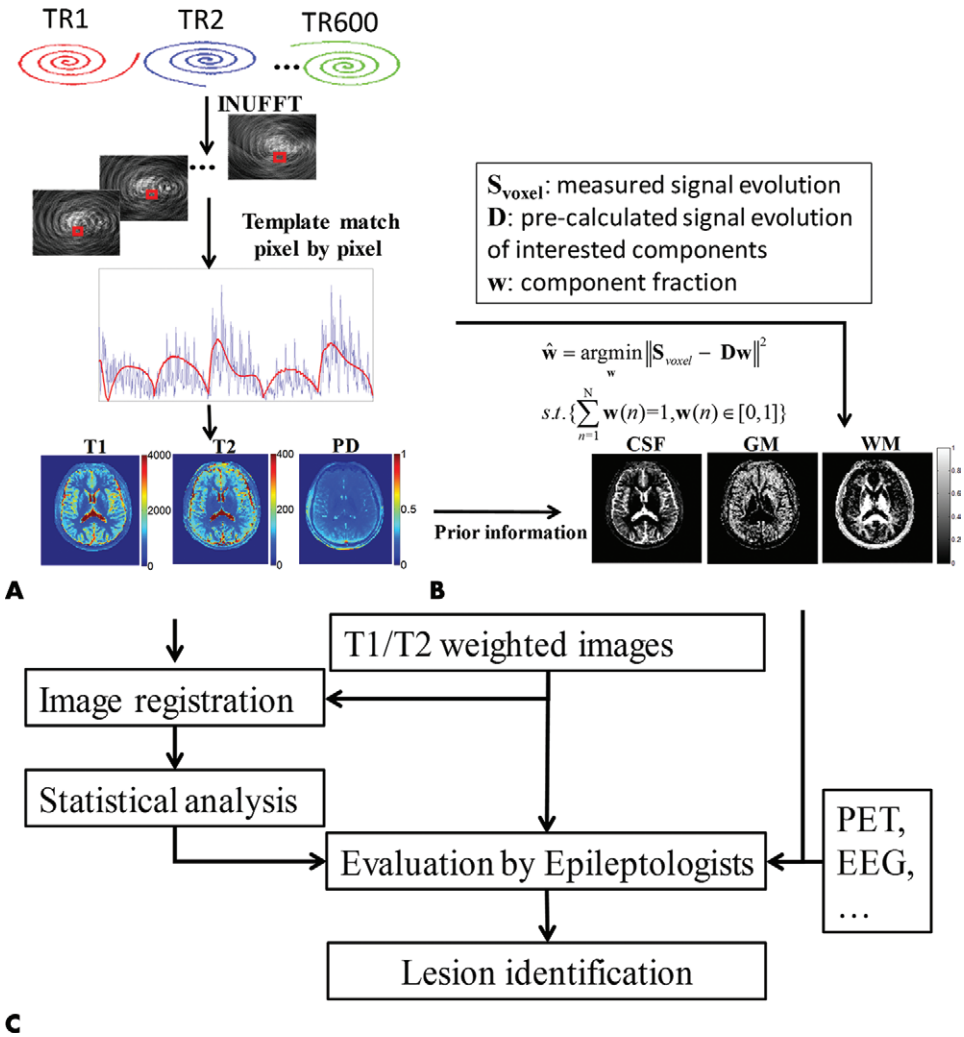

Figure 2: Flowchart shows, *A*, MR fingerprinting and, *B*, regularized tissue-fractional mapping. Flowchart in, *C*, shows the procedure of hippocampal sclerosis (HS) diagnosis. CSF = cerebrospinal fluid, EEG = electroencephalography, GM = gray matter, INUFFT = inverse nonuniform fast Fourier transform, PD = proton density, TR1 = first repetition time, TR2 = second repetition time, TR600 = 600th repetition time, WM = white matter.

Figure 2c shows the procedure of diagnosis of patients with HS and HS lesion identification by using MR fingerprinting. Detailed definitions-based clinical information and imaging analysis are provided in Appendix E1 (online).

Table 2: Demographic Information for Patients with Hippocampus Sclerosis and Corresponding Diagnosis with Extensive Presurgical Work-up, and Routine MR Sequences with and without MR Fingerprinting Analysis

Patient No.	Sex	Age (y)	Disease Duration (y)	Routine MR Finding by Radiologists*	MR Fingerprinting Analysis†	Final Diagnosis‡
S01	F	32	22	L HS	L HS	L HS
S02	F	26	6	Normal	L HS	L HS
S03	F	28	6	L HS	L HS	L HS
S04	F	39	3	R HS	R HS	R HS
S05	F	28	5	L HS	L HS	L HS
S06	F	30	6	Normal	L HS	L HS
S07	F	29	2.5	R HS	R HS	R HS
S08	F	38	8	L HS	Bilateral HS	Bilateral HS
S09	M	42	11	L HS	L HS	L HS
S10	F	16	12	R HS	R HS	R HS
S11	F	50	6	R HS	R HS	R HS
S12	F	27	2.5	L HS	Bilateral HS	Bilateral HS
S13	F	44	3	R HS	R HS	R HS
S14	M	22	10	L HS	L HS	L HS
S15	M	29	4	R HS	R HS	R HS
S16	M	28	5	Normal	L HS	L HS
S17	M	23	4.5	L HS	Bilateral HS	Bilateral HS
S18	M	60	5	L HS	L HS	L HS
S19	F	29	2.5	Normal	L HS	L HS
S20	F	28	3	L HS	L HS	L HS
S21	F	20	3.5	L HS	L HS	L HS
S22	F	43	4	L HS	L HS	L HS
S23	F	30	9	L HS	L HS	L HS
S24	M	25	4	L HS	L HS	L HS
S25	M	44	12	R HS	R HS	R HS
S26	M	31	13	L HS	Bilateral HS	Bilateral HS
S27	F	38	5	R HS	R HS	R HS
S28	F	42	6	L HS	L HS	L HS
S29	F	29	3.5	Normal	Normal	L HS
S30	F	46	9	L HS	L HS	L HS
S31	F	32	15	L HS	Bilateral HS	Bilateral HS
S32	F	22	7	L HS	L HS	L HS
S33	M	27	2.5	L HS	L HS	L HS

Note.—F = female, HS = hippocampal sclerosis, L = left, M = male, R = right.

* Diagnosis rate: 23 of 33; 69.7%.

† Diagnosis rate: 32 of 33; 96.9%.

‡ Final diagnosis is based on extensive presurgical work-ups including electroencephalography (interictal and ictal), semiology, and/or PET.

Statistical Analysis

A group statistical analysis was applied for data from patients and healthy volunteers to validate the effectiveness of T1 and T2 maps obtained at MR fingerprinting for diagnosing HS. The Wilcoxon signed-rank test was used for comparison of T1 and T2 values between manually selected possible HS lesions and contralateral tissue for patients with unilateral HS, and between the left and right hippocampus for healthy control participants. The Wilcoxon rank-sum test was used for comparing the differences between healthy control participants and patients with unilateral MTLE. For patients with bilateral HS, T1 and T2 values of both sides of hippocampus were collected. The statistical difference of bilateral hippocampus was compared with healthy control participants to validate the sensitivity and feasibility of HS diagnosis by using MR fingerprinting method.

Results

Table 2 shows the final diagnosis and detailed disease information of all 33 patients. To date, five patients (identified as S1, S10, S20, S25, and S33) underwent anterior temporal lobectomy and pathologic study–confirmed HS. At final diagnosis, 28 patients were diagnosed with unilateral temporal lobe epilepsy HS (20 left sided and eight right sided in 20 women and eight men; mean age, 33.1 years; age range, 16–60 years) and five were diagnosed with had bilateral TLE-HS (three women and two men; mean age, 30.2 years; age range, 23–38 years). Table 2 also shows lesion detection on the basis of routine MRI without and with MR fingerprinting analysis. Ten of 33 patients were misdiagnosed without MR fingerprinting analysis whereas HS was not detected in one patient (S29) by using MR fingerprinting. The diagnosis rate of MR

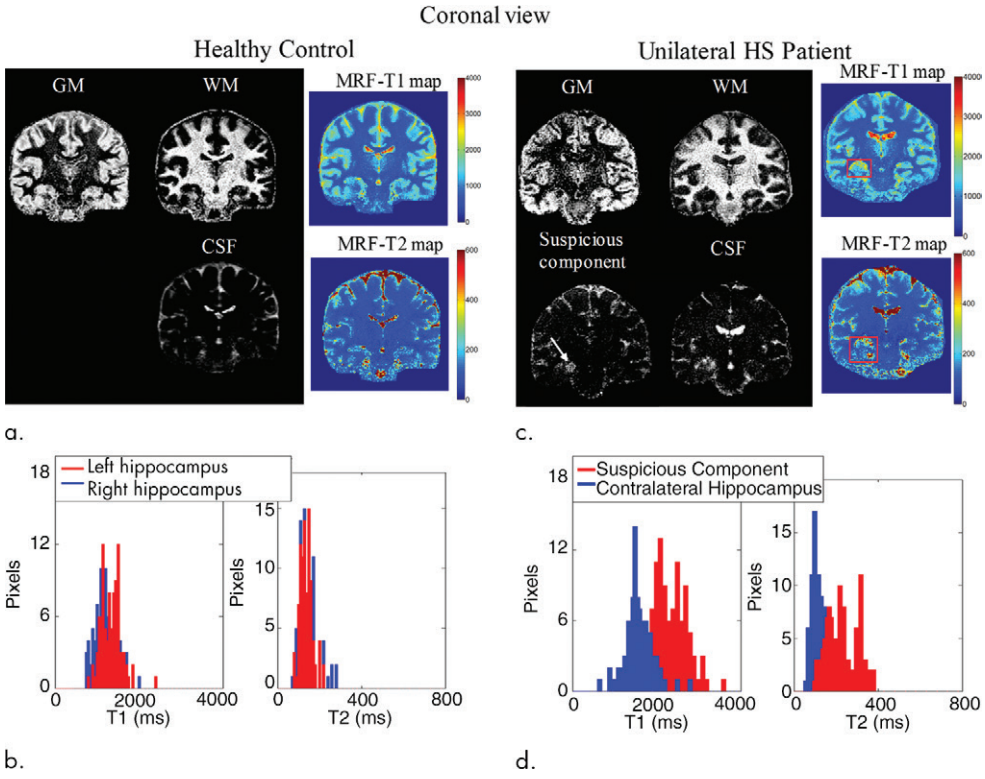

Figure 3: Tissue fraction segmentations in coronal orientation of cerebrospinal fluid (CSF), gray matter (GM), white matter (WM), and suspicious component with MR fingerprinting (MRF) results in **(a)** a healthy control participant (37-year-old man) and **(c)** a typical patient with unilateral hippocampal sclerosis (HS; S25; 44-year-old man); segmented suspicious lesions are shown (arrow in **c**). Histograms of T1 and T2 in the **(b)** healthy control participant and the **(d)** typical patient with unilateral HS are presented.

fingerprinting was 32 of 33 (96.9%; 95% confidence interval: 84.9%, 100%), which indicates improved accuracy and sensitivity of diagnosis ($P = 1.92 \times 10^{-12}$) compared with routine T1- and T2-weighted MR examinations (23 of 33; 69.7%; 95% confidence interval: 51.5%, 81.6%). The majority of the misdiagnoses at routine MRI were from an erroneous diagnosis of bilateral HS as unilateral HS. The 30 healthy control participants were detected at MR fingerprinting with T1 and T2 values in the normal range.

The results of HS lesion identification by using regularized tissue-fraction MR fingerprinting are shown in Figure 3 and Figure E1 (online). Representative sections of MR fingerprinting images acquired from a healthy participant and a patient with unilateral HS and the corresponding tissue-fraction segmentations are shown in both coronal (Fig 3) and transverse (Fig E1 [online]) positions. The abnormal tissue segmentation results of the patient with unilateral HS in segmented suspicious maps show that the separated suspicious components are consistent with possible HS lesions with prolonged relaxation time, indicated by the red boxes in MR fingerprinting T1 and T2 maps. The histogram results of patients with HS demonstrate that mean T1 and T2 values were higher than in the normal hippocampus (1700 msec vs 1310 msec [$P = 8.29 \times 10^{-7}$] for T1 comparison; 148 vs 116 msec [$P = 1.50 \times 10^{-5}$] for T2 comparison), whereas the tissue-fraction maps of healthy participants did not show significant differences between the left and the right hippocampus. The larger volumes of the temporal horn of the lateral ventricle in the segmented cerebrospinal fluid map of the patient with HS shown in Figure 3 reflect the atrophy of hippocampus. All regions suspicious for HS in the 33 recruited patients with HS were marked and identified for subsequent quantitative comparisons.

Figure 4 shows bar plots of T1 and T2 values of 33 patients with MTLE between the left and right hippocampus. The possible T1 and T2 ranges of 30 healthy control participants are demonstrated. Because T1 and T2 values of HS lesions were higher for most of the patients compared with healthy control participants, the likelihood of HS was considered high if one or both hippocampi had T1 and T2 values that were one standard deviation higher than that of healthy control participants. For the 28 patients with unilateral HS, the Wilcoxon signed-rank test between atrophic and contralateral hippocampus ($P = 1.11 \times 10^{-10}$ for T1 comparison and 8.91×10^{-5} for T2 comparison) indicated that T1 and T2 values of the atrophic hippocampus were significantly higher than the contralateral counterpart, whereas there was no significant difference between the left and right hippocampus of healthy control participants ($P = .28$ for T1 comparison and $P = .11$ for T2 comparison). By using the Wilcoxon rank-sum test, no significant differences were found between the contralateral hippocampus of patients with unilateral MTLE and the hippocampus of healthy control participants ($P = .50$ for T1 comparison and $P = .12$ for T2 comparison), whereas there was a significant difference between the atrophic hippocampus of patients with unilateral MTLE and the hippocampus of healthy control participants ($P = 1.11 \times 10^{-10}$ for T1 comparison and 8.91×10^{-5} for T2 comparison).

Table 3 demonstrates the comparison of T1 and T2 values between possible HS lesions and contralateral tissue of 28 patients with unilateral MTLE and the healthy control group. The averaged T1 and T2 values of HS lesions were significantly different from those of normal tissue, whereas those of the contralateral tissue of were within the range of the temporal lobe values of healthy volunteers. For patients with bilateral MTLE (patients S8, S12, S17, S26, and S31), both sides of hippocampus (left HS lesion: T1, 1523 msec ± 259, and T2, 171 msec ± 39; right HS lesion: T1, 1490 msec ± 310, and T2, 182 msec

± 21) had higher T1 and T2 values than healthy control participants (T1, 1249 msec ± 59; T2, 104 msec ± 9).

Figure 5a and Figure E2a (online) show representative sections of the T1-weighted magnetization-prepared rapid gradient echo, T2-weighted fast spin echo, fluid-attenuated inversion recovery, and MR fingerprinting results of two patients with left-sided unilateral MTLE (S14 and S18 in Table 1) in coronal and transverse positions, respectively. Figure 5 and Figure E2 (online) demonstrate T1 (scale, 0–2000 msec) and T2 (scale, 0–150 msec) maps obtained by MR fingerprinting. The box plots of HS and the contralateral hippocampus are displayed in Figure 5b and Figure E2b (online). Both T1 and T2 values of HS lesions were higher than in the contralateral hippocampus. Outliers only appear in the box plot of the HS group, which reflects variations in HS lesions.

Figure 6 displays the results of a patient with bilateral HS (S08 in Table 2) with two adjacent sections shown and their corresponding views of the hippocampus. The sensitivity and accuracy for lesion detection were improved compared with the T1- or T2-weighted images. The diagnosis rate with MR fingerprinting (32 of 33 [96.9%]) improved accuracy and sensitivity of detection by 27.2% compared with conventional MRI protocol (23 of 33 [69.7%]). MR fingerprinting detected image abnormalities that visual inspection failed to identify, thus it is sensitive to subtle relaxometry changes of microstructures such as the hippocampus. The quantitative MR fingerprinting method was shown to improve the diagnosis for patients with unilateral and bilateral HS.

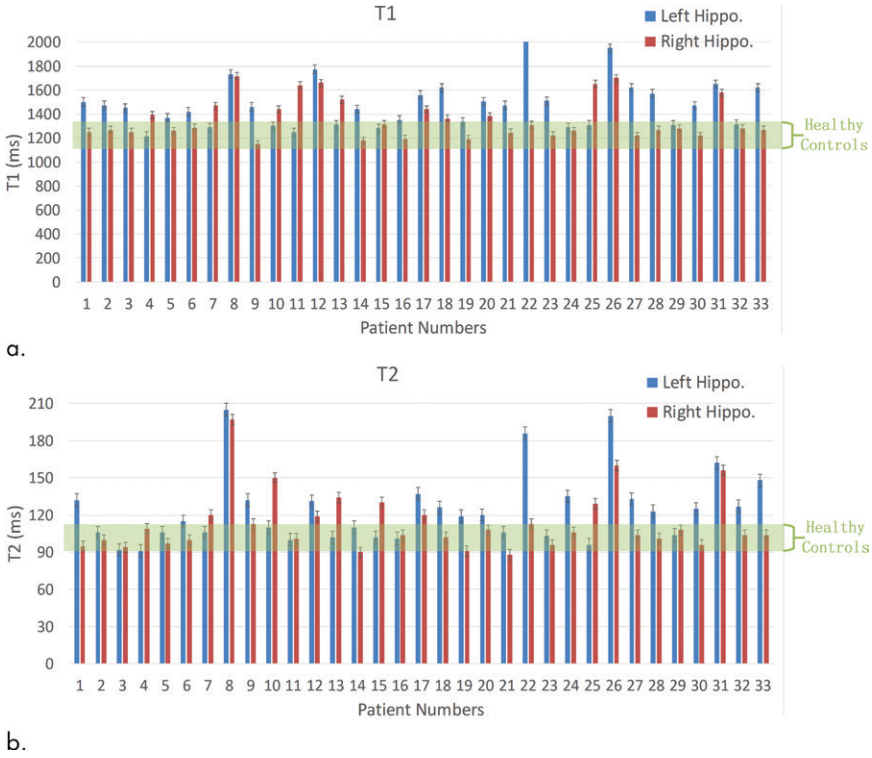

Figure 4: **(a)** T1 and **(b)** T2 bar plots of left (blue) and right (red) hippocampus (hippo.) in 33 patients with mesial temporal lobe epilepsy. The possible T1 and T2 ranges of 30 healthy control participants are shown in the green bars.

Table 3: T1 and T2 Values of Atrophic Hippocampus and Corresponding Contralateral Tissue

Participant	T1 (msec)	T2 (msec)
Atrophic hippocampus (n = 28)*	1361 ± 85	135 ± 15
Contralateral hippocampus (n = 28)*	1255 ± 68	103 ± 11
Healthy control participants (n = 30)	1249 ± 59	104 ± 9

* Patients with unilateral mesial temporal lobe epilepsy.

Discussion

In our study, preliminary results are presented to explore the feasibility of improving the diagnosis of patients with MTLE by using MR fingerprinting. The accuracy and sensitivity of MTLE diagnosis was improved by using MR fingerprinting (96.9%) compared with routine MR visual detection (69.7%). Because of the disease variability of patients with MTLE, the ranges of T1 and T2 values vary among patients.

A recent study (24) showed that MR fingerprinting has high accuracy and repeatability across a wide range of T1 and T2 values. Our previous studies (22,25) also demonstrate the relaxation times estimated by MR fingerprinting to be robust across phantoms and healthy participants compared with the quantification methods (ie, inversion recovery spin-echo acquisition for T1 mapping and spin-echo acquisition for T2 mapping). The T1 and T2 values of healthy control participants in our study were consistent with the literature (3,26), whereas both T1 and T2 values of HS were higher than normal hippocampus. The obtained T1 and T2 maps indicate that MR fingerprinting can differentiate HS from contralateral normal tissue. The group statistical analysis of 28 unilateral HS patients also demonstrates that T2 values are different between HS lesions and contralateral normal tissue, which suggests that MR fingerprinting is reliable and effective for MTLE diagnosis. For subtle changes of bilateral HS lesions, the elevated relaxometry results of both sides of the hippocampus compared with healthy control participants can facilitate diagnostic decision making.

Previous studies (5,27) showed the potential advantages of multicontrast fluid-attenuated inversion recovery, and T1- and T2-weighted multimodal imaging and postprocessing methods to improve detection rate of HS in patients with MTLE. Compared with T1- and T2-weighted images, quantitative measurements of relaxation times are more sensitive and helpful to recognize subtle changes (28,29). In our study, five patients were negative for HS at MRI by using the conventional MRI protocol; their T2 differences between HS lesion and contralateral hippocampus were small. In these patients, T2 maps

alone cannot provide clear evidence for HS detection. However, the significant T1 differences of these five patients helped to improve the visual detection rate. Moreover, MR fingerprinting has the capability of adding more tissue parameters including diffusivity properties (30). Furthermore, the multiparametric maps of MR fingerprinting are recognized simultaneously by template matching with the same image profile, therefore image registration of epilepsy data is not necessary, and signal loss because of interpolation and registration could be reduced. One additional advantage of MR fingerprinting is faster acquisition than conventional quantitative imaging methods. This may lead to a reduction of motion artifacts.

Our study has some limitations. We selected a four-component model for tissue segmentation with a suspicious component marker on the basis of the relaxometry properties of tissues in addition to white matter, gray matter, and cerebrospinal fluid. Although the lesions suspicious for HS can be defined and separated in the map with components suspicious for HS, vessels, eyeball signals, and residual underestimated cerebrospinal fluid fractions may also contaminate the map, which results in a broad distribution of the component outside white matter, gray matter, and poorly defined peaks of T1 and T2 histograms. A four-component model is also limited by the empirical selection of the T1 and T2 values for segmenting the component that is suspicious for HS. We selected the values by observing the abnormal values from T1 and T2 maps that are sensitive to the results of segmentation. In addition, the multiparametric maps used in our study were obtained from undersampled frames, resulting in relatively low signal-to-noise ratio and some incoherent aliasing, which limited the current MR fingerprinting methods to relatively lower in-plane resolution compared with the T1- and T2-weighted images. A possible alternative for the current two-dimensional MR fingerprinting method is a three-dimensional MR fingerprinting acquisition (25,31,32) that provides higher signal-to-noise ratio efficiency and higher image resolution. Another limitation is the underestimation of T1 and T2 values of cerebrospinal fluid because of the simplification of flow effects through frames in the signal model. Recently proposed model-based MR fingerprinting frameworks (33) consider the inflow effects in the dictionary and could supply more accurate estimation in cerebrospinal fluid regions. Our small sample size (33 patients with MTLE and 30 healthy control participants) is also a limitation. Larger and longitudinal studies are needed in the future. Our reference standard definition is another limitation. We cannot be certain that all patients had HS because HS is an intrinsically histopathologic concept. In addition, bilateral HS cannot be proven at histologic analysis because this represents a contraindication for surgery. However, advanced MRI and epilepsy protocols allow the in vivo assumption of HS with high specificity and sensitivity of diagnosis (34,35). In this study, a large section thickness (4 mm) was chosen for fluid-attenuated inversion recovery and T2-weighted images for the signal-to-noise ratio consideration. However, because this section thickness may miss subtle lesions in one plane, a two-plane acquisition is therefore needed to cover the entire temporal lobe of the brain.

MR fingerprinting provides T1 and T2 maps and tissue-fractional maps in a short acquisition time with improved

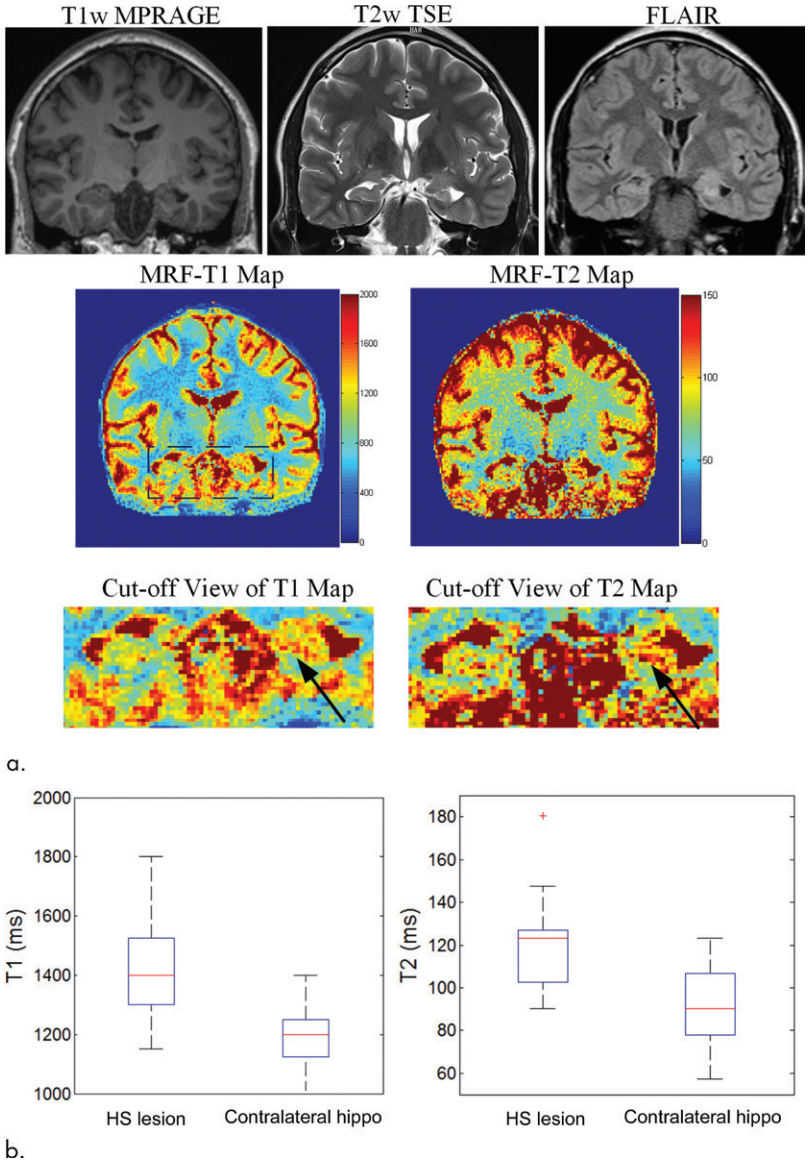

Figure 5: **(a)** Coronal position of T1-weighted magnetization-prepared rapid gradient echo (MPRAGE), T2-weighted fast spin echo (TSE), fluid-attenuated inversion recovery (FLAIR), and T1 and T2 maps obtained by MR fingerprinting (MRF) in a typical patient with unilateral hippocampal sclerosis (HS; S14; 22-year-old man). Arrows on the T1 and T2 maps indicate the possible HS lesions. **(b)** Box-and-whisker plots of HS lesion and contralateral hippocampus (hippo). ms = msec.

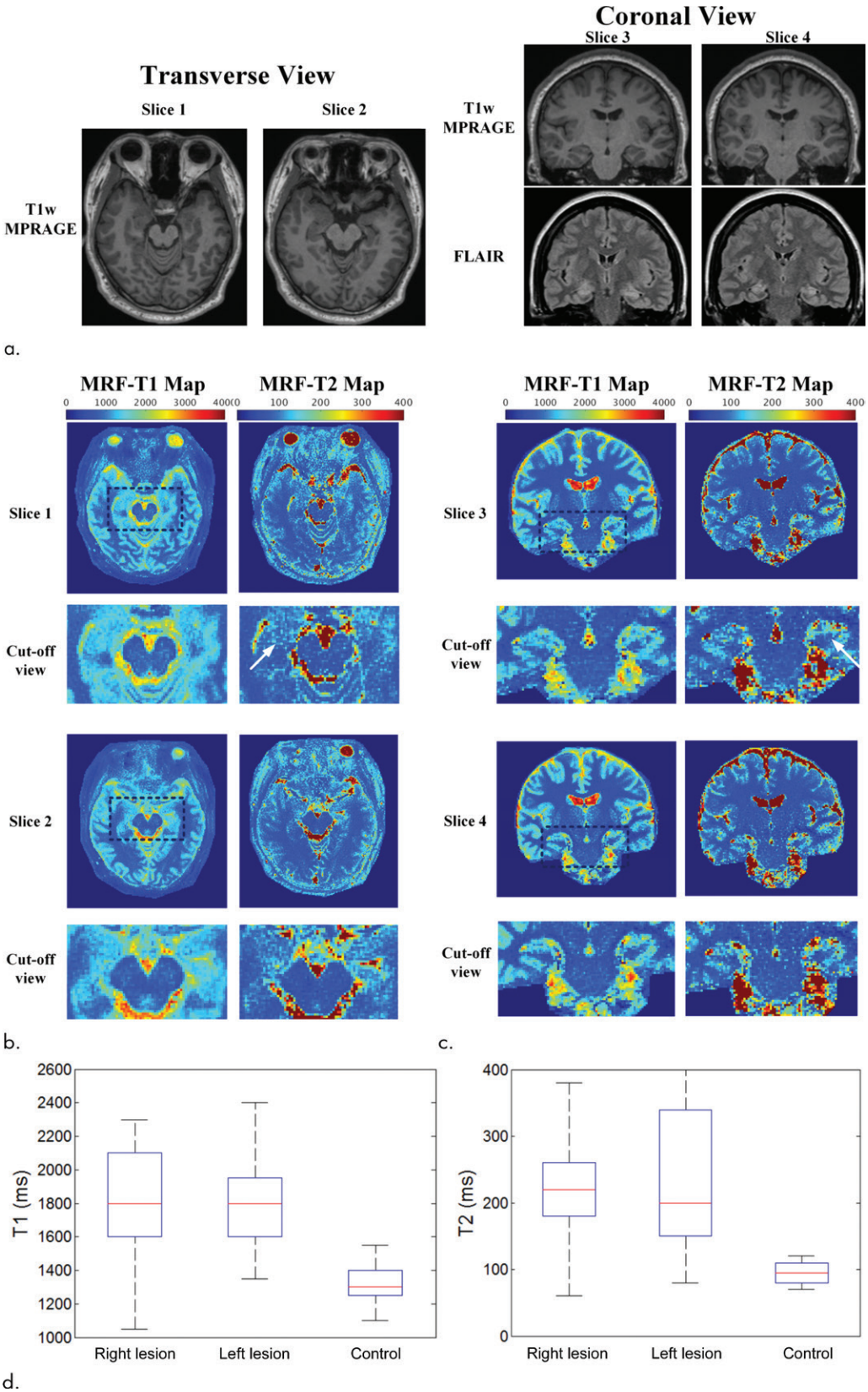

Figure 6: **(a)** Two adjacent sections of fluid-attenuated inversion recovery (FLAIR) images and T1-weighted magnetization-prepared rapid gradient echo (MPRAGE) with transverse and coronal views in a patient with typical bilateral hippocampal sclerosis (S08 in Table 2; 38-year-old woman). MR fingerprinting (MRF) T1 and T2 maps and cut-off views with same **(b)** transverse and **(c)** coronal orientations. Arrows indicate the possible hippocampal sclerosis lesions. **(d)** Box-and-whisker plots of both sides of hippocampal sclerosis lesions and healthy control participants.

accuracy and sensitivity for identification of HS. MR fingerprinting could potentially aid multimodal quantitative mapping and diagnostic decision-making in patients with epilepsy in a clinical setting.

Acknowledgments: We thank Kawin Setsompop, PhD, Berkin Bilgic, PhD, and Mary Kate Manhard, PhD, for helpful discussion and proofreading.

Author contributions: Guarantors of integrity of entire study, C.L., K.W., X.C., Y.L., H.Y., Q.D., H.H., J.Z.; study concepts/study design or data acquisition or data analysis/interpretation, all authors; manuscript drafting or manuscript revision for important intellectual content, all authors; approval of final version of submitted manuscript, all authors; agrees to ensure any questions related to the work are appropriately resolved, all authors; literature research, C.L., K.W., X.C., Y.L., D.W., Q.D., J.Z.; clinical studies, C.L., K.W., X.C., Y.L., D.W., Q.D.; experimental studies, C.L., X.C., Y.L., D.W., H.Y., Q.D., H.H.; statistical analysis, C.L., X.C., Y.L., D.W., Q.D., H.H., J.Z.; and manuscript editing, C.L., K.W., X.C., Y.L., D.W., Q.D., H.H., J.Z.

Disclosures of Conflicts of Interest: **C.L.** disclosed no relevant relationships. **K.W.** disclosed no relevant relationships. **X.C.** disclosed no relevant relationships. **Y.L.** disclosed no relevant relationships. **D.W.** disclosed no relevant relationships. **H.Y.** disclosed no relevant relationships. **Q.D.** disclosed no relevant relationships. **H.H.** disclosed no relevant relationships. **J.Z.** disclosed no relevant relationships.

References

1. Sommer W. Erkrankung des Ammon's Horn als Aetiologis ches Moment der Epilepsien. Arch Psychiatr Nurs 1880;10(3):631–675.
2. Babb TL, Lieb JP, Brown WJ, Pretorius J, Crandall PH. Distribution of pyramidal cell density and hyperexcitability in the epileptic human hippocampal formation. Epilepsia 1984;25(6):721–728.
3. Deoni SC. Magnetic resonance relaxation and quantitative measurement in the brain. In: Modo M, Bulte J, eds. Magnetic resonance neuroimaging: methods in molecular biology (methods and protocols). Vol 711. New York, NY: Humana, 2011; 65–108.
4. Cardinale F, Francione S, Gennari L, et al. SUrface-PRojected FLuid-Attenuation-Inversion-Recovery Analysis: A Novel Tool for Advanced Imaging of Epilepsy. World Neurosurg 2017;98:715–726.e1.
5. Martin P, Bender B, Focke NK. Post-processing of structural MRI for individualized diagnostics. Quant Imaging Med Surg 2015;5(2):188–203.
6. Ashburner J, Friston KJ. Voxel-based morphometry--the methods. Neuroimage 2000;11(6 Pt 1):805–821.
7. House PM, Lanz M, Holst B, Martens T, Stodieck S, Huppertz HJ. Comparison of morphometric analysis based on T1- and T2-weighted MRI data for visualization of focal cortical dysplasia. Epilepsy Res 2013;106(3):403–409.
8. Braga B, Yasuda CL, Cendes F. White Matter Atrophy in Patients with Mesial Temporal Lobe Epilepsy: Voxel-Based Morphometry Analysis of T1- and T2-Weighted MR Images. Radiol Res Pract 2012;2012(5):481378.
9. Focke NK, Symms MR, Burdett JL, Duncan JS. Voxel-based analysis of whole brain FLAIR at 3T detects focal cortical dysplasia. Epilepsia 2008;49(5):786–793.
10. Focke NK, Yogarajah M, Bonelli SB, Bartlett PA, Symms MR, Duncan JS. Voxel-based diffusion tensor imaging in patients with mesial temporal lobe epilepsy and hippocampal sclerosis. Neuroimage 2008;40(2):728–737.
11. Bernasconi A, Bernasconi N, Caramanos Z, et al. T2 relaxometry can lateralize mesial temporal lobe epilepsy in patients with normal MRI. Neuroimage 2000;12(6):739–746.
12. Conlon P, Trimble MR, Rogers D, Callicott C. Magnetic resonance imaging in epilepsy: a controlled study. Epilepsy Res 1988;2(1):37–43.
13. Woermann FG, Barker GJ, Birnie KD, Meencke HJ, Duncan JS. Regional changes in hippocampal T2 relaxation and volume: a quantitative magnetic resonance imaging study of hippocampal sclerosis. J Neurol Neurosurg Psychiatry 1998;65(5):656–664.
14. Ma D, Gulani V, Seiberlich N, et al. Magnetic resonance fingerprinting. Nature 2013;495(7440):187–192.
15. Hamilton JI, Jiang Y, Ma D, et al. Cardiac MR fingerprinting for T1 and T2 mapping in four heartbeats. J Cardiovasc Magn Reson 2016;18(Suppl 1):W1.
16. Chen Y, Jiang Y, Pahwa S, et al. MR fingerprinting for rapid quantitative abdominal imaging. Radiology 2016;279(1):278–286.
17. Badve C, Yu A, Ma D, et al. Magnetic resonance fingerprinting of brain tumors: initial clinical results. Neuro Oncol 2014;16(Suppl 5):v139.
18. Yu AC, Badve C, Ponsky LE, et al. Development of a combined MR fingerprinting and diffusion examination for prostate cancer. Radiology 2017;283(3):729–738.
19. Deshmane AV, Ma D, Jiang Y, et al. Validation of Tissue Characterization in Mixed Voxels Using MR Fingerprinting [abstr]. In: Proceedings of the Twenty-Second Meeting of the International Society for Magnetic Resonance in Medicine. Berkeley, Calif: International Society for Magnetic Resonance in Medicine, 2014; 94.
20. McGivney D, Deshmane A, Jiang Y, et al. Bayesian estimation of multicomponent relaxation parameters in magnetic resonance fingerprinting. Magn Reson Med 2018;80(1):159–170.
21. Jiang Y, Ma D, Seiberlich N, Gulani V, Griswold MA. MR fingerprinting using fast imaging with steady state precession (FISP) with spiral readout. Magn Reson Med 2015;74(6):1621–1631.
22. Cao X, Liao C, Wang Z, et al. Robust sliding-window reconstruction for Accelerating the acquisition of MR fingerprinting. Magn Reson Med 2017;78(4):1579–1588.
23. Cao X, Liao C, Wang Z, et al. An improved tissue-fraction MR Fingerprinting(TF-MRF) with additional fractional regularization [abstr]. In: Proceedings of the Twenty-Fourth Meeting of the International Society for Magnetic Resonance in Medicine. Berkeley, Calif: International Society for Magnetic Resonance in Medicine, 2016; 4223.
24. Jiang Y, Ma D, Keenan KE, Stupic KF, Gulani V, Griswold MA. Repeatability of magnetic resonance fingerprinting T1 and T2 estimates assessed using the ISMRM/NIST MRI system phantom. Magn Reson Med 2017;78(4):1452–1457.
25. Liao C, Bilgic B, Manhard MK, et al. 3D MR fingerprinting with accelerated stack-of-spirals and hybrid sliding-window and GRAPPA reconstruction. Neuroimage 2017;162:13–22.
26. Wansapura JP, Holland SK, Dunn RS, Ball WS Jr. NMR relaxation times in the human brain at 3.0 tesla. J Magn Reson Imaging 1999;9(4):531–538.
27. Maehara T. Neuroimaging of epilepsy. Neuropathology 2007;27(6):585–593.
28. Jackson GD, Connelly A, Duncan JS, Grünewald RA, Gadian DG. Detection of hippocampal pathology in intractable partial epilepsy: increased sensitivity with quantitative magnetic resonance T2 relaxometry. Neurology 1993;43(9):1793–1799.
29. Sato S, Iwasaki M, Suzuki H, et al. T2 relaxometry improves detection of non-sclerotic epileptogenic hippocampus. Epilepsy Res 2016;126:1–9.
30. Warntjes JB, Dahlqvist O, Lundberg P. Novel method for rapid, simultaneous T1, T2*, and proton density quantification. Magn Reson Med 2007;57(3):528–537.
31. Ma D, Jiang Y, Chen Y, et al. Fast 3D magnetic resonance fingerprinting for a whole-brain coverage. Magn Reson Med 2018;79(4):2190–2197.
32. Buonincontri G, Sawiak SJ. MR fingerprinting with simultaneous B1 estimation. Magn Reson Med 2016;76(4):1127–1135.
33. Cao X, Liao C, Wang Z, et al. A model-based velocity mapping of blood flow using MR fingerprinting [abstr]. In: Proceedings of the Twenty-Fifth Meeting of the International Society for Magnetic Resonance in Medicine. Berkeley, Calif: International Society for Magnetic Resonance in Medicine, 2017; 941.
34. Jackson GD, Berkovic SF, Tress BM, Kalnins RM, Fabinyi GC, Bladin PF. Hippocampal sclerosis can be reliably detected by magnetic resonance imaging. Neurology 1990;40(12):1869–1875.
35. Kuzniecky RI, Bilir E, Gilliam F, et al. Multimodality MRI in mesial temporal sclerosis: relative sensitivity and specificity. Neurology 1997;49(3):774–778. * Patients with unilateral mesial temporal lobe epilepsy.